Biomarker Records from Core GH02-1030 off Tokachi in the Northwestern Pacific over the Last 23,000 Years; Environmental Changes during the Last Deglaciation

Masaki Inagaki[1,2], Masanobu Yamamoto[1,*], Yaeko Igarashi[3] and Ken Ikehara[4]

[1]*Faculty of Environmental Earth Science, Hokkaido University, Sapporo 060-0810, Japan*

[2]*Present; Yamamoto Building Co., Ltd., 3-3-1-3 Toyooka, Asahikawa, Hokkaido 078-8233, Japan*

[3]*Institute for Paleoenvironment of Northern Regions, Koyocho 3-7-5, Kitahiroshima, 061-1134, Japan*

[4]*Geological Survey of Japan, AIST, Tsukuba, Ibaraki 305-8567, Japan*

*Corresponding author; Phone/Fax: +81-11-706-2379, E-mail: myama@ees.hokudai.ac.jp (M. Yamamoto)

Short title: Paleoenvironment in the NW Pacific

Abstract:

We investigated marine and terrestrial environmental changes at the northern Japan margin in the northwestern Pacific during the last 23,000 years by analyzing biomarkers (alkenones, long-chain *n*-alkanes, long-chain *n*-fatty acids, and lignin-derived materials) in Core GH02-1030. The $U^{K'}_{37}$-derived temperature in the last

glacial maximum (LGM) centered at 21 ka was ~10˚C, which was 2˚C lower than the core-top temperature (~12˚C). This small temperature drop does not agree with pollen evidence of a large air temperature drop (more than 4˚C) in the Tokachi area. This disagreement might be attributed to a bias of $U^{K'}_{37}$-derived temperature within 2.5˚C by a seasonal shift in alkenone production. The $U^{K'}_{37}$-derived temperature was significantly low during the last deglaciation. Because this cooling was significant in the Kuroshio-Oyashio transition zone, the temperature drops are attributable to the southward displacement of the Kuroshio-Oyashio boundary. Abundant lignin-derived materials, long-chain *n*-alkanes and long-chain *n*-fatty acids indicate a higher contribution of terrigenous organic matter from 17 to 12 ka. This phenomenon might have resulted from an enhanced coastal erosion of terrestrial soils due to marine transgression and/or an efficient inflow of higher plant debris to river waters from 17 to 12 ka.

Keywords: North Pacific, Japan, East Asia, biomarker, glacial, deglacial, paleoenvironment, paleotemperature.

1. Introduction

The last glacial period (~117–12 ka) ended with the last deglaciation (Termination I; ~19–7 ka). The onset of sea-surface warming varied in different regimes (in the Pacific, reviewed by Kiefer and Kienast, 2005). The mid-latitude northwestern Pacific is one of the regions of the globe where deglacial warming occurred latest at Termination I (e.g., Oba and Murayama, 2004; Yamamoto *et al*., 2004; 2005b). A pollen study demonstrated the southward expansion of open taiga vegetation known as the

48 "Kenbuchi Stadial" on the central Hokkaido Island during the last deglaciation (Igarashi,
49 1996). An earlier study also showed several cooling events during the last deglaciation
50 on southwestern Hokkaido (Sakaguchi, 1989).

51 The region contains the subarctic boundary between the subtropical Kuroshio and
52 subarctic Oyashio currents (Fig. 1) and is sensitive to global climate changes (e.g.,
53 Chinzei *et al*., 1987; Isono *et al*., 2009). Early studies have roughly reconstructed that
54 the Kuroshio-Oyashio boundary shifted southward during the last glacial period and
55 northward during the last interglacial period from ~129 to ~117 ka (e.g., Moore *et al*.,
56 1980; Thompson and Shackleton, 1980; Chinzei *et al*., 1987; Harada *et al*., 2004).
57 Yamamoto *et al*. (2005b), however, demonstrated drops in $U^{K'}_{37}$-derived temperature in
58 Core MD01-2421 off the coast of central Japan from ~17 to ~12 ka during the last
59 deglaciation, which was attributed to a southward shift of the summer position of
60 Kuroshio-Oyashio boundary due to the weaker North Pacific High and stronger
61 Okhotsk High. These cooling intervals were not consistent with a global warming trend
62 during the last deglaciation.

63 We generated the records of $U^{K'}_{37}$-derived temperatures and terrestrial and marine
64 biomarkers during the last 23 kyr from Core GH02-1030 taken off the southeastern
65 coast of Hokkaido Island in the northwestern Pacific. We examined both marine and
66 terrestrial environmental changes at the northern Japan margin in order to elucidate the
67 climate linkage between the ocean and land. The high sedimentation rate (average 29
68 cm/kyr) allowed us to perform a much higher resolution analysis than in previous
69 studies.

70

71 **2. Study site**

72 The study site is located at the northern edge of the mixing zone between Oyashio
73 and Kuroshio waters (Fig. 1). Cold and warm mesoscale eddies from the Oyashio and
74 Kuroshio develop in the mixing zone. The Kuroshio-Oyashio boundary is displaced
75 seasonally. The southern limit of the Oyashio stays at ~38.5°N in April, gradually shifts
76 northward to ~40°N until October, and then moves more rapidly northward to ~41.5°N
77 to December before gradually returning southward until April (Data from Japan
78 Meteorological Agency, http://www.data.kishou.go.jp/kaiyou/
79 db/hakodate/knowledge/oyashio.html) The monthly mean sea-surface temperature
80 (SST) ranges from 2.4°C in March to ~18.6°C in August and averages ~9.7°C
81 (Reynolds *et al*., 2002). The seasonal SST change reflects both the latitudinal
82 displacement of the Kuroshio-Oyashio boundary and the development of thermal
83 stratification. Thermal stratification develops from summer to fall in this region.
84 The SST in the Kuroshio-Oyashio transition zone is also influenced by decadal
85 oscillations of two oceanic gyre circulations: the Pacific Decadal Oscillation (PDO;
86 Mantua *et al*., 1997; Minobe, 1997) and the North Pacific Gyre Oscillation (NPGO; Di
87 Lorenzo *et al*., 2008). The PDO and NPGO modes of climate variability emerge from
88 analyses of North Pacific SST anomalies (the leading principal component) and
89 sea-surface height anomalies (the second principal component), respectively (Mantua *et*
90 *al*., 1997; Di Lorenzo *et al*., 2008). The PDO represents changes in the subpolar gyre
91 circulation, while the NPGO represents changes in the subtropical gyre and the
92 northernmost Alaskan gyre circulation (Di Lorenzo *et al*., 2008). Both oscillations show
93 El Niño-like spatial patterns of SSTs, and are linked to El Niño-Southern Oscillation
94 (Dettinger *et al*., 2001; Di Lorenzo *et al*., 2008).
95 The spatial distribution of organic matter in surfacial sediments off Tokachi

(42°–43°N, 143.5°–145°E) was described in Usui *et al*. (2006). According to Usui *et al*. (2006), total organic carbon (TOC) content is variable on the continental shelf and depends on the influx of terrigenous organic matter from the Tokachi River (Usui *et al*., 2006). The Tokachi River (156 km length) flows through the Tokachi plains and empties into the northwestern Pacific. River flow increases in spring and early fall due to snowmelt and an increase of precipitation, respectively. On the continental slope, the organic matter derives mainly from marine organisms. The TOC increases with increasing depth, is maximized at ~1100 m, and then decreases to 2000 m. The TOC was significantly correlated with silt and clay content, suggesting that transport and deposition of organic-rich fine sediment particles by hydrodynamic processes were major factors controlling TOC off Tokachi (Usui *et al*., 2006).

3. Materials and methods

A piston core GH02-1030 (8.14 m long) was collected offshore of the southeastern coast of Hokkaido Island at 42°13.77′N, 144°12.53′E at a water depth of 1212 m in 2002 during the *R/V Daini-Hakurei-Maru* GH02 cruise (Fig. 1). Sediments in this core consisted of olive-gray silty clay and clayey silt with sand seams at 454.5–456.5 and 609–611 cm (Fig. 2). The uppermost and middle parts of the core were diatomaceous. Visual observation and soft-X-ray radiographs revealed no clear erosion surface in the core. Very weak lamination was found at two horizons in the middle part of the core, and coarser sandy silt existed between the two laminated horizons (Ikehara *et al*., 2006).

The age model was established using data from Ikehara *et al*. (2006). The age model between 10.31 and 21.84 ka was created by the AMS ^{14}C ages of 13 samples of planktonic foraminifera; *Neogloboquadrina pachyderma* or mixed planktonic

120 foraminifera, mainly *N. pachyderma* with minor portions of *Globigerina bulloides*. The
121 age model after 10.31 ka was created by the AMS ^{14}C ages of four samples of mixed
122 benthic foraminifera. The conventional age of benthic foraminifera was converted to the
123 planktonic value by subtracting 700±151 years, which is equivalent to the average
124 difference in conventional ages between planktonic and benthic foraminifera in samples
125 at depths of 2.10, 2.20, and 2.35 m (Ikehara *et al*., 2006). The calendar age was
126 converted using the CALIB5.0 program and the Marine04.14C dataset (Reimer *et al*.,
127 2004) with a 776-year reservoir correction (DR = 376±46 years; Kuzmin *et al*., 2001)
128 (Fig. 3).
129 The analysis of alkenones and *n*-alkanes was conducted following the modified
130 method of Yamamoto *et al*. (2000). Sediment sample (2 g in dry weight) was extracted
131 twice at 100°C under 1000 psi with 11 mL of dichloromethane/methanol (6/4 v/v) using
132 a DIONEX accelerated solvent extractor ASE-200. The lipid extract was separated into
133 four fractions (F1: 3 mL of hexane; F2: 3 mL of hexane/toluene [3/1 v/v]; F3: 4 mL of
134 toluene; F4: 3 mL of toluene/methanol [3/1 v/v]) by column chromatography (SiO_2 with
135 5% distilled water, 5.5 mm ID × 45 mm long). *n*-$C_{24}D_{50}$ and *n*-$C_{36}H_{74}$ were added as
136 internal standards into the F1 and F3 fractions, respectively. Gas chromatography for
137 the F1 and F3 fractions was conducted using a Hewlett Packard 6890 gas
138 chromatograph (GC) with on-column injection and electronic pressure control systems
139 and a flame ionization detector. The column used was a capillary column coated with
140 Chrompack CP-Sil5CB (60 m ID × 0.25 mm, 0.25 μm coating). The oven
141 temperature was programmed from 70 to 130°C at 20°C/min, from 130 to 310°C at
142 4°C/min, and then was held at 310°C for 30 min in the analysis of the F1 fraction. The
143 oven temperature was programmed from 70 to 290°C at 20°C/min, from 290 to 310°C

144 at 0.5°C/min, and then was held at 310°C for 60 min in the analysis of the F3 fraction.
145 Helium was used as a carrier gas, and the flow velocity was maintained at 30 cm/s.
146 The alkenone unsaturation index $U_{37}^{K'}$ was calculated from the concentrations of di- and
147 tri-unsaturated C_{37} alken-2-ones (C_{37}MK) using the expression (Brassell *et al*., 1986):
148 $U_{37}^{K'}$ = [$C_{37:2}$MK]/([$C_{37:2}$MK] + [$C_{37:3}$MK]). The calculation of temperature was
149 conducted according to the equation: Temperature (°C) = ($U_{37}^{K'}$ – 0.039)/0.034, based on
150 an experimental result for cultured strain 55a of *Emiliania huxleyi* (Prahl *et al*., 1988),
151 within an analytical accuracy of 0.24°C.
152 The fatty acids and lignin were analyzed following the methods of Yamamoto *et*
153 *al*. (2001) and Yamamoto *et al*. (2005a) modified after S. Yamamoto (2000),
154 respectively. Pyrolysis gas chromatography-mass spectrometry with *in situ* methylation
155 with tetramethylammonium hydroxide (TMAH-pyrolysis-GC/MS) was carried out
156 using a Japan Analytical Industry JHP-5 Curie point pyrolyzer that was directly
157 connected to the injection port of a Hewlett Packard 5973 gas chromatograph-mass
158 selective detector. The column used was a Chrompack CP-Sil5CB (length, 30 m; i.d.,
159 0.25 mm; thickness, 0.25 μm). The sediment sample (ca. 20 mg) was placed on a Ni-Co
160 pyrofoil plate with 30 μl of 5% TMAH in methanol and 20 μl of internal standard
161 solution (0.1 g/L *n*-nonadecanoic acid in hexane). The methanol and hexane were dried
162 in room temperature, and the sample was wrapped in pyrofoil. The sample was heated
163 at 590°C for 20 sec in the pyrolyzer, and the generated compounds were transferred to
164 the GC splitless injection system at 300°C with a helium carrier gas. The oven
165 temperature was programmed from 70 to 310°C at 4°C/min after the initial hold time of
166 1 min, and then it was held isothermally at 310°C for 30 min. The mass spectrometer
167 was run in the full scan ion-monitoring mode (*m/z* 50–650). Electron impact spectra

were obtained at 70 eV. Identification of *n*-fatty acids and lignin phenols was achieved by comparison of their mass spectra and retention times with those of authentic standards. The standard deviations in three duplicate analyses averaged 13% of the concentration for total fatty acids. The standard deviations in replicate analysis (five times) were 10, 7, 15, and 8% of the concentration for total syringyl phenol (S), total vanillyl phenols (V), total cinnamyl phenol (C), and total eight lignin (Σ8; S+V+C), respectively, and they were 0.01, 0.03, and 0.06 for S/V and C/V ratios and the ratio of acid to aldehyde of vanyllyl phenol [$(Ad/Al)_v$ ratio], respectively.

Total organic carbon content was measured following the method of Yamamoto (2004) using a LECO WR-112 carbon analyzer. The analyzer was attached to a halogen trap (antimony and potassium iodide). To remove carbonate carbon, the sample was acidified according to the following procedure. The sample (~0.1 g) was soaked in 1-M HCl solution in a ceramic crucible overnight and was heated at 110°C for 3 hr after adding new 1-M HCl. The sample was rinsed to remove chlorides by twice adding pure water, and was heated again at 110°C for 3 hr. The precision of measurement was better than 0.01 wt%.

4. Results

4.1. Total organic carbon contents

Total organic carbon (TOC) content varied between 0.4 and 2.0 wt% of dry sediment, with an average of 1.1 wt% (Fig. 4A), and showed a decreasing trend with increasing depth. Maximal peaks of TOC content were observed at ~14.2 and ~4.4 ka.

4.2. Alkenones and $U^{K'}_{37}$-derived temperature

192 Total concentration of $C_{37:2}$ and $C_{37:3}$ alkenones ranged from 0.06 to 2.09
193 mg/g-sediment, with an average of 0.67 mg/g-sediment. The concentration abruptly
194 increased at ~14.5 ka (Fig. 4B). The average concentrations before and after 15 ka were
195 0.22 and 1.20 mg/g of sediment, respectively, and the concentration level rose 5.5 times
196 at 15 ka.
197 The temperature varied between 7.4 and 14.4˚C during the last 23 kyr (Fig. 4C).
198 The temperature during the Last Glacial Maximum (LGM) centered at 21 ka was ~10˚C,
199 which was 2˚C lower than the core-top temperature (~12˚C) at the study site (Fig. 4C).
200 The temperature decreased to ~8˚C at 16 ka with a high fluctuation of ~1˚C in
201 amplitude, in correlation with the North Atlantic Oldest Dryas cold period. The
202 temperature increased to ~12˚C at 14.7 ka, in correlation with the North Atlantic
203 Bølling-Allerød warm period. The temperature subsequently decreased and reached
204 ~9˚C at ~12.1 ka, which was correlated with the North Atlantic Younger Dryas cold
205 period. The temperature abruptly increased to ~12˚C at 11.3 ka, dropped to 9˚C at 10.1
206 ka and then rose again to ~12˚C at 9.6 ka. The temperature gradually increased and
207 maximized at ~6.9 ka and then decreased up to the late Holocene.
208
209 **4.3. Normal fatty acids**
210 Total concentrations of short-chain C_{14}-C_{18} *n*-fatty acids, derived mainly from
211 marine organisms, showed two maxima at 15 ka and 11 ka (Fig. 4D). The total
212 concentrations of long-chain C_{26}-C_{30} *n*-fatty acids, derived predominantly from higher
213 plants (Kvenvolden *et al.*, 1967), were significantly higher from 17.5 to 12 ka than
214 those in other intervals (Fig. 4E). The abundance ratios of long-chain to short-chain
215 fatty acids, an index of terrestrial organic matter contribution, showed a similar

variation as that of long-chain fatty acid concentration (Fig. 4F).

4.4. Normal alkanes

Normal-alkanes showed a monomodal homologous distribution with a maximum at C_{29}. Their homologous distribution is typical of terrestrial higher plant waxes (Eglinton and Hamilton, 1967). Total concentrations of long-chain *n*-C_{27}, C_{29} and C_{31} alkanes, derived from higher plants, tended to be higher from 17.5 to 9 ka than in other intervals (Fig. 4G). The odd/even carbon preference index (CPI) of long-chain C_{24}-C_{34} *n*-alkanes, defined by Bray and Evans (1961), ranged from 2.2 to 6.3, with an average of 4.4. Most values were in the typical range of fresh *n*-alkanes from higher plants. We observed several spikes of low CPI from 17 to 11 ka (Fig. 4H), implying the contribution of mature (thermally altered) terrestrial organic matter.

4.5. Lignin abundance and composition

$\Sigma 8$ (mg/10g-sediment, defined by Hedges and Mann, 1979a), which is the total amount of eight lignin phenols belonging to vanillyl (vanillin, acetovanillone, and vanillic acid), syringyl (syringaldehyde, acetosyringone, and syringic acid) and cinnamyl groups (*p*-coumaric acid and ferulic acid), varied between 0.009 and 0.202, with an average of 0.062 (Fig. 4I). Λ (mg/100mg-TOC), which is the total amount (in mg) of the above-mentioned eight lignin phenols in 100 mg of TOC (Hedges and Mann, 1979a), varied between 0.008 and 0.259, with an average of 0.063 (Fig. 4J). $\Sigma 8$ and Λ were higher from 18.4 to 17.2 ka and from 15.4 to 12.5 ka than during the other intervals (Figs. 4I and 4J). The $\Sigma 8$ and Λ were much smaller than those of riverine particles from the Tokachi River in Hokkaido onshore of the study site ($\Sigma 8$ = 0.13–0.88

240 and Λ = 0.69–2.94, n = 4, M. Inagaki, unpublished data), implying that the organic
241 matter in the core is mainly of marine origin.

242 The ratios of syringyl (S) to vanillyl (V) phenols (S/V ratio) and of cinnamyl (C)
243 to vanillyl (V) phenols (C/V ratio) were used for the assessment of paleovegetation (e.g.,
244 Hedges and Mann, 1979b; Goñi and Hedges, 1992). The S/V ratio, which is a
245 contribution index of angiosperms relative to gymnosperms (Hedges and Mann, 1979b),
246 ranged from 0.06 to 0.65, with an average of 0.29 (Fig. 4K). The values fell within the
247 range of mixture of angiosperms and gymnosperms (S/V = 0.9-4 and 0, respectively;
248 Hedges and Mann, 1979b). The S/V ratios were generally higher in the LGM and the
249 early Holocene than in the last deglaciation and the middle and late Holocene (Fig. 4K).

250 In Core GH02-1030, cinnamyl phenol was hardly detected in lignin-lean samples,
251 only detected samples are shown in Fig. 4L. In the detected samples, the C/V ratio
252 ranged from 0.19 to 0.88, with an average of 0.42. The C/V ratio is used as an index to
253 present the contribution of nonwoody tissues and herbs (Hedges and Mann, 1979b).
254 Recently, Ishiwatari *et al*. (2006) found high C/V (>1) and Pc/Vc (>10) ratios in
255 sediments from Lake Baikal, which they attributed to the contribution of pollen lignin.
256 In Core GH02-1030, no correlation was observed between the C/V ratio and pollen
257 abundance (Y. Igarashi, unpublished data), and PC/Vc [p-coumaric acid/ferulic acid]
258 ratios (0.1-0.7) were much lower than those of pollen (>10; Ishiwatari *et al*., 2006),
259 implying that the contribution of pollen lignin was not important in the study core.

260

261 **5. Discussion**

262 **5.1. Sea surface temperatures during the Last Glacial Maximum**

263 The $U^{K'}_{37}$-derived temperature record from Core GH02-1030 is characterized by

264 relatively warm temperatures during the LGM (Fig. 5A). The temperature in the LGM
265 centered at 21 ka was ~10˚C, which was 2˚C lower than the core-top temperature
266 (~12˚C). Even warmer temperatures during the LGM than the Holocene were observed
267 at other locations in the subpolar region of northwestern Pacific margins such as the
268 sites of Cores PC-2, PC-4, and MD01-2412 in the Sea of Okhotsk (Fig. 5B; Seki *et al*.,
269 2004; Harada *et al*., 2006a), and Cores PC-9 and MD01-2408 in the Sea of Japan (Fig.
270 5B; Ishiwatari *et al*., 2001). Ishiwatari *et al*. (2001) interpreted the warm temperatures
271 during the LGM in the Sea of Japan as resulting from the combination of a shift of the
272 alkenone production season and a well-developed thermal stratification. Seki *et al*.
273 (2004) attributed warm temperatures at Cores PC-2 and PC-4 in the Sea of Okhotsk
274 during the LGM partly to the shift of the alkenone production season from October to
275 August. Recently, Fujine *et al*. (2006) found a shorter-chain alkenone ($C_{36:2}$
276 ethlylalkenone) and alkenoate ($C_{36:2}$ ethyalkenoate) in Core MD01-2408 (the Sea of
277 Japan) during the last two glacial periods (~9–57 and ~129–164 ka). The occurrence of
278 these unique compounds was associated with low salinity and anomalously high
279 $U^{K'}_{37}$-derived temperatures. This correspondence implies either physiological stress
280 induced by low salinity or that a genotypic difference in alkenone producers caused the
281 anomalously high $U^{K'}_{37}$ values during the last two glacial periods in the Sea of Japan
282 (Fujine *et al*., 2006). Our survey indicated an absence of these shorter-chain alkenone
283 and alkenoate in samples from Core GH012-1030, which indicates that the temperatures
284 during the LGM at the study site were not affected by low salinity events.
285 The study site is characterized by a large seasonal sea surface temperature (SST)
286 variation. SST varies between 2.4˚C in March and 18.6˚C in August (Reynolds *et al*.,
287 2002). The core-top $U^{K'}_{37}$-derived temperature at the study site was 11.9˚C (Fig. 5A),

288 corresponding to the SST in June and was higher than the annual mean SST at the study
289 site (9.7˚C; Reynolds *et al*., 2002). A time-series sediment-trap study demonstrated that
290 alkenones are continuously produced from April to October and the production is
291 optimal in July at 39˚N, 147˚E in the mid-latitude northwestern Pacific (Yamamoto *et*
292 *al*., 2007). The $U^{K'}_{37}$-derived temperature in summer indicate a thermocline temperature
293 that is at most 6˚C lower than the SST (Yamamoto *et al*., 2007). Lower $U^{K'}_{37}$-derived
294 temperatures than SST in summer were also observed at other locations in the
295 mid-latitude North Pacific (Station JT-2; Sawada *et al*., 1998, Stations KNOT, 40N and
296 50N; Harada *et al*., 2006b).

297 We predicted a possible increase in the $U^{K'}_{37}$-derived temperature when the onset
298 of alkenone production was delayed based on the one-year sediment-trap data of the
299 flux-weighted $U^{K'}_{37}$-derived temperature at 39˚N, 147˚E in 1998 (Site WCT-2;
300 Yamamoto *et al*., 2007). The delay in the onset of alkenone production by 1 month
301 (early May onset) induced only a 0.1˚C rise and delays 2 (early June), 3 (late June), 4
302 (late July), 5 (late August), or 6 (late September) months resulted in a total increase in
303 $U^{K'}_{37}$-derived temperatures of 0.7˚C, 0.9˚C, 2.1˚C, 2.2˚C, and 2.5˚C, respectively (Fig. 6).
304 This calculation implies that $U^{K'}_{37}$-derived temperature can be biased by up to 2.5˚C
305 when the onset of alkenone production shifts from April to September.

306 A sediment-trap study at a cooler site (50˚N, 165˚E) demonstrated a short period
307 of alkenone production in October and November (Harada *et al*., 2006b). The seasonal
308 shift of haptophyte blooms is presumably caused by the temperature dependence of the
309 growth rates of these algae, which was demonstrated by culture experiments (Conte *et*
310 *al*., 1998). These observations support our hypothesis that the $U^{K'}_{37}$-derived temperature

311 during the LGM was biased within 2.5˚C by a seasonal shift in alkenone production.

312 Pollen analysis indicated abundant *Larix* during the LGM in Core GH02-1030 (Y.
313 Igarashi, unpublished data). The southern limit of *Larix* is south Sakhalin Island in the
314 modern natural flora (e.g., Igarashi and Igarashi, 1998). The July temperature at
315 Korsakov in south Sakhalin is 14.8˚C (Japan Weather Association, 1982), but 18.3˚C at
316 Obihiro in the Tokachi area, onshore of the study site (National Astronomical
317 Observatory, 2000); the temperature difference is thus ~4˚C. This suggests that the
318 summer air temperature in the Tokachi area during the LGM was more than 4˚C lower
319 than that at present. This air temperature drop was larger than the drop of the
320 $U^{K'}_{37}$-derived temperature (~ 2˚C). If there was no seasonal shift of alkenone production,
321 the difference suggests the mismatch of temperature changes between atmosphere and
322 ocean surface. If there was a seasonal shift, the difference in SST between the LGM and
323 present is possibly a maximum of 4.5˚C, which agrees with the estimated difference in
324 air temperature (>4˚C).
325

326 **5.2. Cooling during the last deglaciation**

327 The $U^{K'}_{37}$-derived temperature record from Core GH02-1030 is characterized by
328 cooling events during the last deglaciation from 17 to 10 ka (Fig. 5A). The general trend
329 in $U^{K'}_{37}$-derived temperatures is consistent with that of foraminiferal Mg/Ca-based
330 temperatures (Sagawa and Ikehara, 2008). The temperatures were even lower than those
331 during the LGM. The seasonal shift in alkenone production less likely enhanced a
332 temperature drop, because alkenone producers prefer warmer water (Conte *et al*., 1998),
333 but mutes the drop by shifting the production to a warmer season. The seasonal shift of
334 alkenone production was, therefore, less likely to account for the cooling during the last

335 deglaciation.

336 Igarashi (1996) reported a cooling event in central Hokkaido Island during the last
337 deglacial, based on abundant *Larix* pollen in terrestrial boring cores, which she called
338 the “Kenbuchi Stadial”. This stadial was not precisely defined in age by Igarashi (1996).
339 Pollen analysis for Core MD01-2421 indicated that the terrestrial vegetation was
340 *Larix-Picea* forest in the LGM from 22 to 18.5 ka and changed to open *Larix-Picea*
341 forest from 18.5 to 14.8 ka, *Betula* forest from 14.8 to 11.0 ka, mixed forest with *Larix*
342 from 11.0 to 8.5 ka, and mixed forest after 8.5 ka (Fig. 4N). *Larix* dominated in the
343 LGM and continued to be present from 18.5 to 8.5 ka. In contrast to terrestrial boring
344 cores from central Hokkaido (Igarashi, 1996), pollen record from Core GH02-1030 did
345 not show a “Kenbuchi stadial”-like cold reversal during the last deglaciation, but
346 showed a slow and gradual warming from 15 to 9 ka (Yaeko Igarashi, unpublished data).
347 Cooler sea surface temperatures during the last deglaciation at Core GH02-1030 might
348 be related to this slow warming on land.

349 The variation of $U^{K'}_{37}$-derived temperature in Core GH02-1030 during the last 23
350 kyr was nearly parallel to that in Core MD01-2421 (Yamamoto *et al*., 2005b; Isono *et*
351 *al*., 2009) off central Japan and Core PC-6 (Minoshima *et al*., 2007) off northeastern
352 Japan (Fig. 5A). Since these sites are located in the Kuroshio-Oyashio transition, the
353 temperature variations are attributable to the latitudinal displacement of the
354 Kuroshio-Oyashio boundary. The southward displacement of the Kuroshio-Oyashio
355 boundary resulted in cooler temperatures during the last deglaciation at the study site.

356 Yamamoto *et al*. (2005b) attributed a strong cooling at MD01-2421 off central
357 Japan during the last deglaciation to both the depressed North Pacific High and the
358 enhanced Okhotsk High. Recently Yamamoto (2009) revisited the data of Yamamoto *et*

359 *al*. (2004; 2005b) and interpreted that the cooling at the Japan margin during the last
360 deglaciation was caused by the decline of subtropical gyre circulation which is linked to
361 changes in tropical ocean-atmosphere dynamics.

362 In modern climate, the summer Okhotsk High is enhanced by the summer heating
363 of northeastern Siberia, north of the Sea of Okhotsk, and the northerly cold air
364 advection to the south of the Okhotsk High generates cold SST anomalies in the
365 Kuroshio-Oyashio transition (Ogi *et al*., 2004). The enhanced heating of the land
366 surface over northeastern Siberia due to increasing summer insolation and atmospheric
367 greenhouse gases, might have resulted in the stronger summer Okhotsk High during the
368 last deglaciation (Yamamoto *et al*., 2005b). This cooling by northerly winds from the
369 Okhotsk High might contribute to low SST in addition to the southward displacement of
370 the Kuroshio-Oyashio boundary during the last deglaciation.

371

372 **5.3. Increased influx of terrigenous organic matter during the last deglaciation**

373 High abundance of lignin, long-chain *n*-alkanes, and long-chain *n*-fatty acids
374 indicate the enhanced contribution of terrigenous organic matter during the last
375 deglaciation from 17 to 12 ka (Figs. 4E, 4G and 4I). A similar phenomenon was
376 observed in the Sea of Okhotsk (Ternois *et al*., 2001; Seki *et al*., 2003). This
377 phenomenon was attributed to the enhanced transportation of terrigenous organic matter
378 by ice rafts (Ternois *et al*., 2001) and subsequently to the increase in reworked
379 terrigenous organic matter from the continental shelves of the northern margin because
380 ice rafts decreased during the last deglaciation in the Sea of Okhotsk (Seki *et al*., 2003).

381 Ad/Al_v [vanillic acid/vanillin] and Ad/Al_s [syringic acid/acetosyringone] ratios are
382 indices of aerobic microbial degradation in freshwater environment (Goñi *et al*., 1993).

383 Fresh, moderately degraded, and highly degraded lignin have Ad/Al_v ratios of ~0.5, ~3,
384 and 7–12, respectively, in the TMAH procedure (Hatcher *et al*., 1995). In Core
385 GH02-1030, the Ad/Al_v values ranged from 0.3 to 6.2, with an average of 2.3 (Fig. 4M).
386 This suggests that the lignin was not highly degraded but slightly or moderately
387 degraded by aerobic microbes. Relatively high values were observed from ~19 to ~7 ka
388 (Fig.4M), implying the transportation of more degraded terrigenous organic matter into
389 the study site.

390 Spikes of low CPI appeared from 17 to 11 ka (Fig. 4H). Since CPI decreases with
391 increasing thermal maturity in sedimentary rock (e.g., Philipi, 1965), the spikes of low
392 CPI in the last deglacial samples indicate the contribution of mature sedimentary
393 organic matter. This suggests that Tertiary sedimentary rocks exposed in the Tokachi
394 district onshore of the study site were eroded and mature organic matter was transported
395 to the study site during the last deglaciation.

396 Two possible processes may have increased the inflow of terrestrial organic matter
397 during the last deglaciation. Firstly, an enhanced coastal erosion due to marine
398 transgression likely increased terrestrial organic matter. The sea level rose more than
399 120 m from 19 to 6 ka (Fig. 4O, Lambeck *et al*., 2002). Oguri *et al*. (2000) found a
400 negative excursion of carbon isotopes of bulk organic matter in a core from the
401 Okinawa Trough in the East China Sea. They attributed this phenomenon to enhanced
402 coastal erosion during the last deglaciation. Seki *et al*. (2003) interpreted a similar
403 phenomenon in the Sea of Okhotsk as being due to the same mechanism. The average
404 rate of sea level rise was ~1 cm/yr during the last deglaciation, and such a rapid rise
405 could have enhanced coastal erosion. This hypothesis is consistent with the increases in
406 mature sedimentary organic matter and more degraded terrestrial organic matter during

407 the last deglaciation, which were observed in the study core.

408 Secondly, more likely, the development of an alluvial plain in the Tokachi area
409 during the last deglaciation also could have increased the discharge of terrestrial organic
410 matter to the study site (Fig. 7). Geomorphological studies of river terraces on the
411 Tokachi district onshore of the study site demonstrated a contrast of fluvial
412 accumulation-incision balance between the upper and lower reaches of the rivers during
413 the LGM and the Holocene (Hirakawa and Ono, 1974; Hirakawa, 1977). Fluvial
414 deposits accumulated in the upper and middle reaches of the rivers, and the plain was
415 incised in the lower reaches due to low sea level stand during the LGM. During the
416 Holocene, mountainous regions were incised, presumably due to increased precipitation,
417 and thick sediments accumulated in the alluvial fan. Grain size analysis for Core
418 GH02-1030 showed that the sand fraction was significant in the LGM interval and
419 disappeared in the overlying intervals (Ikehara *et al*., 2006). This change likely reflected
420 the landward shift of the deposition center of terrestrial detrital matter as a result of sea
421 level rise, which is also consistent with the change in mass balance from incision to
422 accumulation in the lower reach of the Tokachi River.

423 The suspended organic matter in the rivers of Hokkaido Island, including the
424 Tokachi River, is fed mainly by riverbank erosion (Alam *et al*., 2007; Alam, personal
425 communication). During the LGM, the Tokachi Plain was incised; since the rivers
426 flowed within the valley, organic matter was not efficiently supplied from the vegetation
427 on the plain (Fig. 7). Mountainous regions were less vegetated (Ono and Hirakawa,
428 1975) and could not supply substantial higher-plant debris to the river waters. During
429 the last deglaciation, the alluvial plain developed as a result of sea level rise, and
430 organic matter was efficiently fed to rivers from the bank erosion by meandering rivers

(Fig. 7). The presence of altered lignin and mature organic matter in this interval suggests that the reworking process of terrestrial organic matter was more important during this period than other periods. During the Holocene, the deposition center shifted landward, and the transportation of terrestrial organic matter to the study site decreased (Fig. 7).

6. Conclusions

The $U^{K'}_{37}$-derived temperature record from Core GH02-1030 is characterized by relatively warm temperatures during the LGM. The temperature in the LGM centered at 21 ka was ~10˚C, which was 2˚C lower than the core-top temperature (~12˚C). An evaluation based on modern sediment trap data suggests that $U^{K'}_{37}$-derived temperature can be biased by up to 2.5˚C when the onset of alkenone production shifts from April to September. If there was the seasonal shift of alkenone production, the difference in SST between the LGM and present is possibly a maximum of 4.5˚C, which agrees with the difference in air temperature (>4˚C) estimated from pollen assemnbages.

The $U^{K'}_{37}$-derived temperature record from Core GH02-1030 is characterized by cooling events during the last deglaciation (Fig. 5A). These cooling events are correlated with the “Kenbuchi Stadial” previously reported from pollen records of inland Hokkaido (Igarashi, 1996). The variation of $U^{K'}_{37}$-derived temperature in Core GH02-1030 was nearly parallel to those off the coast of central and northeastern Japan. The southward displacement of the Kuroshio-Oyashio boundary resulted in cooler temperatures during the last deglaciation.

High abundance of lignin, long-chain *n*-alkanes and long-chain *n*-fatty acids indicate the enhanced contribution of terrigenous organic matter during the last

455 deglaciation from 17 to 12 ka. High Ad/Al_v [vanillic acid/vanillin] and Ad/Al_s [syringic
456 acid/acetosyringone] ratios and the spikes of low CPI (odd/even carbon number
457 preference of long-chain *n*-alkanes) indicate the contribution of more degraded and
458 mature (thermally altered) organic matter. This presumably reflected an enhanced
459 coastal erosion of terrestrial soils due to marine transgression and/or an efficient inflow
460 of higher plant debris to river waters during this period.
461
462 **Acknowledgements**
463 We thank Yutaka Ichikawa, Takuya Sagawa, Osamu Seki, Seiya Nagao, Masao
464 Minagawa, Tomohisa Irino, Tadamichi Oba, Takeshi Nakatsuka, Kazuomi Hirakawa,
465 Yugo Ono (Hokkaido University), Shuichi Yamamoto (Soka University), Takuya Itaki,
466 Atsushi Noda, Hajime Katayama (Geological Survey of Japan, AIST), and the
467 shipboard scientists of the GH02 cruise for their valuable input. Comments by Ryoshi
468 Ishiwatari, Naomi Harada, and the anonymous reviewer improved this manuscript. This
469 study was carried out under Grants-in-Aid for Scientific Research (B) No. 16340158
470 and Scientific Research (A) No. 19204051 of JSPS (MY).
471
472 **References**
473 Alam, M.J., S. Nagao, T. Aramaki, Y. Shibata and M. Yoneda (2007): Transport of
474 particulate organic matter in the Ishikari River, Japan during spring and summer.
475 *Nucl. Instr. Meth. Phys. Res. B,* **259**, 513–517.
476 Bray, E.E. and E.D. Evans (1961): Distribution of *n*-paraffins as a clue to the
477 recognition of source beds. *Geochim. Cosmochim. Acta,* **22**, 2–9.
478 Chinzei, K, K. Fujioka, H. Kitazato, I. Koizumi, T. Oba, M. Oda, H. Okada, T. Sakai

and Y. Tanimura (1987): Postglacial environmental change of the Pacific Ocean off the coasts of central Japan. *Mar. Micropal.,* **11**, 273–291.

Conte, M.H., A. Thompson, D. Lesley and R.P. Harris (1998): Genetic and physiological influences on the alkenone/alkenoate versus growth temperature relationship in *Emiliania huxleyi* and *Gephyrocapsa oceanica*. *Geochim. Cosmochim. Acta,* **62**, 51-68.

Dettinger, M.D., D.S. Battisti, R.D. Garreaud, G.J. McCabe, Jr. and C.M. Bitz (2001): Interhemispheric effects of interannual and decadal ENSO-like climate variations on the Americas. p. 1-16. In *Interhemispheric Climate Linkages,* Academic Press, San Diego.

Di Lorenzo, E., N. Schneider, K.M. Cobb, P.J.S. Franks, K. Chhak, AJ. Miller, J.C. McWilliams, S.J. Bograd, H. Arango, E. Curchitser, T.M. Powell and P. Rivière (2008): North Pacific Gyre Oscillation links ocean climate and ecosystem change. *Geophys. Res. Let.,* **35**, L08607.

Eglinton, G. and R.J. Hamilton (1967): Leaf epicuticular waxes. *Science,* **156**, 1322-1355.

Fujine, K., M. Yamamoto, R. Tada and Y. Kido (2006): A salinity-related occurrence of a novel alkenone and alkenoate in Late Pleistocene sediments from the Japan Sea. *Org. Geochem.,* **37**, 1074-1084.

Goñi, M.A. and J.I. Hedges (1992): Lignin dimers: Structures, distribution, and potential geochemical applications. *Geochim. Cosmochim. Acta,* **56**, 4025-4043.

Goñi, M.A., B. Nelson, R.A. Blanchette and J.I. Hedges (1993): Fungal degradation of wood lignins: Geochemical perspectives from CuO-derived phenolic dimers and monomers. *Geochim. Cosmochim. Acta,* **57**, 3985-4002.

503 Harada, N., N. Ahagon, M. Uchida and M. Murayama (2004): Northward and
504 southward migrations of frontal zones during the past 40 kyr in the
505 Kuroshio-Oyashio transition area. *Geochem. Geophys. Geosyst.,* **5**, Q09004.
506 Harada, N., N. Ahagon, T. Sakamoto, M. Uchida, M. Ikehara and Y. Shibahara (2006a):
507 Rapid fluctuation of alkenone temperature in the southwestern Okhotsk Sea during
508 the past 120 ky. *Global Planet. Change,* **55**, 29-46.
509 Harada, N., M. Sato, A. Shiraishi and M.C. Honda (2006b): Characteristics of alkenone
510 distributions in suspended and sinking particles in the northwestern North Pacific.
511 *Geochim. Cosmochim. Acta,* **70**, 2045-2062.
512 Hatcher, P.G., M.A. Nanny, R.D. Minard, S.D. Dible and D.M. Carson (1995):
513 Comparison of two thermochemolytic methods for the analysis of lignin in
514 decomposing gymnosperm wood: the CuO oxidation method and the method of
515 thermochemolysis with tetramethylammonium hydroxide (TMAH). *Org.*
516 *Geochem.,* **23**, 881-888.
517 Hedges, J.I. and D.C. Mann (1979a): The lignin geochemistry of marine sediments from
518 the southern Washington coast. *Geochim. Cosmochim. Acta,* **43**, 1809-1918.
519 Hedges, J.I. and D.C. Mann (1979b): The characterization of plant tissues by their
520 lignin oxidation products. *Geochim. Cosmochim. Acta,* **43,** 1803-1807.
521 Hirakawa, K. and Y. Ono (1974): The landform evolution of the Tokachi Plain.
522 *Geograph. Rev. Japan,* **47**, 607-632 (in Japanese).
523 Hirakawa, K. (1977): Chronology and evolution of landforms during the late
524 Quaternary in the Tokachi Plain and adjacent areas, Hokkaido, Japan. *Catena,* **4**,
525 255-288.
526 Igarashi, Y. (1996): A late glacial climate reversion in Hokkaido, Northeast Asia,

527 inferred from the *Larix* pollen record. *Quat. Sci. Rev.,* **15**, 989-995.
528 Igarashi, Y. and T. Igarashi (1998): Late Holocene vegetation history in south Sakhalin,
529 northeast Asia. *Jpn. J. Ecol.,* **48**, 231-244 (in Japanese).
530 Ikehara, K., K. Ohkushi, A. Shibahara and M. Hoshiba (2006): Change of bottom water
531 conditions at intermediate depths of the Oyashio region, NW Pacific over the past
532 20,000 yrs. *Global Planet. Change,* **53**, 78-91.
533 Ishiwatari, R., M. Houtatsu and H. Okada (2001): Alkenone-sea surface temperatures in
534 the Japan Sea over the past 36 kyrs: Warm temperatures at the last glacial
535 maximum. *Org. Geochem.,* **32**, 57-67.
536 Ishiwatari, R., S. Yamamoto and S. Shimoyama (2006): Lignin and fatty acid records in
537 Lake Baikal sediments over the last 130 kyr: A comparison with pollen records.
538 *Org. Geochem.,* **37**, 1787-1802.
539 Isono, D., M. Yamamoto, T. Irino, T. Oba, M. Murayama, T. Nakamura and H.
540 Kawahata (2009): The 1,500-year climate oscillation in the mid-latitude North
541 Pacific during the Holocene. *Geology*, 37, 591-594.
542 Japan Weather Association (1982): *Climate of Hokkaido*. Japan Weather Association,
543 Hokkaido Headquater, Sapporo, 319p (in Japanese).
544 Kiefer, T. and M. Kienast (2005): Patterns of deglacial warming in the Pacific Ocean: a
545 review with emphasis on the time interval of Heinrich event. *Quat. Sci. Rev.,* **24**,
546 1063–1081.
547 Kuzmin, Y.V., G.S. Burr and A.J.T. Jull (2001): Radiocarbon reservoir correction ages in
548 the Peter the Great Gulf, Sea of Japan, and eastern coast of the Kunasir, Southern
549 Kurils (Northwestern Pacific). *Radiocarbon,* **43**, 477-481.
550 Kvenvolden, K.A. (1967): Normal fatty acids in sediments. *J Amer. Oil Chem. Soc.,* **44**,

628-636.

Lambeck, K., Y. Yokoyama and T. Purcell (2002): Into and out of the Last Glacial Maximum: sea level change during Oxygen Isotope Stages 3 and 2. *Quat. Sci. Rev.*, **21**, 343-360.

Mantua, N.J., S.R. Hare, Y. Zhang, J.M. Wallace and R.C. Francis (1997): A Pacific interdecadal climate oscillation with impacts on salmon production. *Bull. Amer. Meteorol. Soc.*, **78**, 1069-1079.

Minobe, S. (1997): A 50-70 year climate oscillation over the North Pacific and North America. *Geophys. Res. Let.*, **24**, 683-686.

Minoshima, K., H. Kawahata and K. Ikehara (2007): Changes in biological production in the mixed water region (MWR) of the northwestern North Pacific during the last 27 kyr. *Palaeogeogr., Palaeoclimatol., Palaeoecol.*, **254**, 430-447.

Moore, T.C., L.H. Burkle, K. Geitzenauer, K., *et al*. (1980): The reconstruction of sea surface temperatures in the Pacific Ocean of 18,000 B.P. *Mar. Micropal.*, **5**, 215-247.

National Astronomical Observatory (2000): *Chronological Scientific tables 2001*. Maruzen, Tokyo, 1064p (in Japanese).

Oba, T. and M. Murayama (2004): Sea surface temperature and salinity changes in the northwest Pacific since the last glacial maximum. *J. Quat. Sci.*, **19**, 1-12.

Ogi, M., Y. Tachibana and K. Yamazaki (2004): The connectivity of the winter North Atlantic Oscillation (NAO) and the summer Okhotsk High. *J. Meteorol. Soc. Japan*, **82**, 905-913.

Oguri, K., E. Matsumoto, Y. Saito, M.C. Honda, N. Harada and M. Kusakabe (2000): Evidence for the offshore transport of terrestrial organic matter due to the rise of

575 sea level: The case of the East China Sea continental shelf. *Geophys. Res. Let.,* **27**,
576 3893-3896.
577 Ono, Y. and K. Hirakawa (1975): Glacial and periglacial morphogenetic environments
578 around the Hidaka Range in the Würm glacial age. *Geograph. Rev. Japan,* **48**,
579 1-26.
580 Philipi, G.T. (1965): On the depth, time and mechanism of petroleum generation.
581 *Geochim. Cosmochim. Acta,* **29**, 1021-1049.
582 Prahl, F.G., L.A. Muehlhausen and D.L. Zahnle (1988): Further evaluation of long-chain
583 alkenones as indicators of paleoceanographic conditions. *Geochim. Cosmochim.*
584 *Acta,* **52**, 2303-2310.
585 Reimer, P.J., *et al*. (2004): IntCal04 Terrestrial radiocarbon age calibration, 26 - 0 ka
586 BP. *Radiocarbon,* **46**, 1029-1058.
587 Reynolds, R.W., N.A. Rayner, T.M. Smith, D.C. Stokes and W. Wang (2002): An
588 improved in situ and satellite SST analysis for climate. *J. Climate* **15**, 1609-1625.
589 Sagawa, T. and K. Ikehara (2008): Intermediate water ventilation change in the
590 subarctic northwest Pacific during the last deglaciation. *Geophys. Res. Let.*, **35**,
591 L24702, doi:10.1029/2008GL035133.
592 Sakaguchi, Y. (1989): Some pollen records from Hokkaido and Sakhalin. *Bull. Dpt.*
593 *Geography, Univ. Tokyo,* **21**, 1-17.
594 Sawada, K., N. Handa and T. Nakatsuka (1998): Production and transport of long-chain
595 alkenones and alkyl alkenoates in a sea water column in the northwestern Pacific
596 off central Japan. *Mar. Chem.,* **59**, 219-234.
597 Seki, O., K. Kawamura, T. Nakatsuka, K. Ohnishi, M. Ikehara and M. Wakatsuchi
598 (2003): Sediment core profiles of long-chain *n*-alkanes in the Sea of Okhotsk:

599 Enhanced transport of terrestrial organic matter from the last deglaciation to the
600 early Holocene. *Geophys. Res. Let.,* **30**, 1001.
601 Seki, O, K. Kawamura, M. Ikehara, T. Nakatsuka and T. Oba (2004): Variation of
602 alkenone sea surface temperature in the Sea of Okhotsk over the last 85 kyrs. *Org.*
603 *Geochem.,* **35**, 347-354.
604 Ternois, Y., K. Kawamura, L. Keigwin, N. Ohkouchi and T. Nakatsuka (2001): A
605 biomarker approach for assessing marine and terrigenous inputs to the sediments of
606 Sea of Okhotsk for the last 27,000 years. *Geochim. Cosmochim. Acta,* **65**, 791-802.
607 Thompson, P.R. and N.J. Shackleton (1980): North Pacific paleoceanography: late
608 Quaternary coiling variations of planktonic foraminifer *Neogloboquadrina*
609 *pachyderma*. *Nature,* **287**, 829-833.
610 Usui, T., S. Nagao, M. Yamamoto, K. Suzuki, I. Kudo, S. Montani, A. Noda and M.
611 Minagawa (2006): Distribution and sources of organic matter in surficial sediments
612 on the shelf and slope off Tokachi, western North Pacific, inferred from C and N
613 stable isotopes and C/N ratios. *Mar. Chem.,* **98**, 241–259.
614 Yamamoto, S. (2000): A basic investigation for high resolution analysis of
615 paleo-climatic changes by the tetramethyl ammonium hydroxide (TMAH) method.
616 *Bull. Faculty Education, Soka Univ.,* **49**, 61-78 (in Japanese).
617 Yamamoto, M., M. Yamamuro and R. Tada (2000): Late Quaternary records of organic
618 carbon, calcium carbonate and biomarkers from Site 1016 off Point Conception,
619 California margin. *Proc. ODP, Sci. Res.,* **167**, 183-194.
620 Yamamoto, M., H. Kayanne and M. Yamamuro (2001): Characteristics of organic
621 matter in lagoonal sediments from the Great Barrier Reef. *Geochem. J.,* **35**,
622 385-401.

623 Yamamoto, M. (2004): Data Report: Organic carbon, and alkenone sea-surface
624 temperature from Sites 1175, 1176, and 1178, Nankai Trough. *Proc. ODP, Sci. Res.,*
625 **190**, 196, 1-10.
626 Yamamoto, M., T. Oba, J. Shimamune and T. Ueshima (2004): Orbital-scale anti-phase
627 variation of sea surface temperature in mid-latitude North Pacific margins during
628 the last 145,000 years. *Geophys. Res. Let.,* **31**, L16311,
629 doi:10.1029/2004GL020138.
630 Yamamoto, M., Y. Ichikawa, Y. Igarashi and T. Oba (2005a): Late Quaternary variation
631 of lignin composition in Core MD012421 off central Japan, NW Pacific.
632 *Palaeogeogr., Palaeoclimatol., Palaeoecol.,* **229**, 179-186.
633 Yamamoto, M., R. Suemune and T. Oba (2005b): Equatorward shift of the subarctic
634 boundary in the northwestern Pacific during the last deglaciation. *Geophys. Res.*
635 *Let.,* **32**, L05609, doi:10.1029/2004GL0201903.
636 Yamamoto, M., A. Shimamoto, T. Fukuhara, H. Naraoka, Y. Tanaka and A. Nishimura
637 (2007): Seasonal and depth variations in molecular and isotopic alkenone
638 composition of sinking particles from the western North Pacific. *Deep-Sea Res. I,*
639 **54**, 1571-1592.
640 Yamamoto, M. (2009): Response of mid-latitude North Pacific surface temperatures to
641 orbital forcing and linkage to the East Asian summer monsoon and tropical
642 ocean-atmosphere interactions. *J. Quat. Sci.*, in press.
643

644 **Figure captions**

645 Fig. 1. Map showing the locations of Core GH02-1030, previously studied core sites
646 (PC-2 and PC4; Seki *et al*., 2004, MD01-2412; Harada *et al*., 2006a, PC-6; Minoshima
647 *et al*., 2007, MD01-2421; Yamamoto *et al*., 2005b; PC-9; Ishiwatari *et al*., 2001,
648 MD01-2408; Fujine *et al*., 2006) and sediment trap sites (JT-2; Sawada *et al*., 2998,
649 KNOT, 50N and 40N; Harada *et al*., 2006b, WCT-2; Yamamoto *et al*., 2007).

650

651 Fig. 2. Stratigraphic column of Core GH02-1030 (Ikehara *et al*., 2006).

652

653 Fig. 3. Age-depth model of Core GH02-1030. Open circles indicate the samples that
654 were not used for the age-depth model.

655

656 Fig. 4. Changes in (A) total organic carbon (TOC), (B) $C_{37:2}$ and $C_{37:3}$ alkenone
657 concentrations, (C) $U^{K'}_{37}$-derived temperature, (D) the concentrations of short-chain
658 *n*-C_{14}-C_{18} fatty acids (SCFAs) and (E) long-chain *n*-C_{26}-C_{30} fatty acids (LCFAs), (F) the
659 ratio of LCFAs to SCFAs (LCFA/SCFA), (G) long-chain C_{27}, C_{29}, and C_{31} *n*-alkane
660 concentration and (H) the carbon preference index of *n*-alkanes (C_{24}-C_{34}; CPI_{NA}), in (I)
661 Σ8, (J) Λ, (K) S/V, (L) C/V, (M) Ad/Al (solid circle = Ad/Al_v; open circle = Ad/Al_s), (N)
662 vegetation pattern reconstructed based on pollen assemblages (Yaeko Igarashi,
663 unpublished data), and (O) reconstructed sea level (Lambeck *et al*., 2002) in Core
664 GH02-1030 during the last 23,000 years. YD = Younger Dryas period, BA =
665 Bølling-Allerød period, OD = Oldest Dryas period, and LGM = Last Glacial Maximum.

666

667 Fig. 5. (A) Alkenone temperature records from Core GH02-1030 during the last 23,000

668 years and those off northeastern Japan (PC-6; Minoshima *et al*., 2007) and off central
669 Japan (MD01-2421; Yamamoto *et al*., 2005b; Isono *et al*., 2009). (B) Alkenone
670 temperature records from the Sea of Okhotsk (PC-2 and PC4; Seki *et al*., 2004,
671 MD01-2412; Harada *et al*., 2006a) and those in the Sea of Japan (PC-9; Ishiwatari *et al*.,
672 2001, MD01-2408; Fujine *et al*., 2006) during the last 23,000 years. The temperatures
673 were calculated using an equation obtained by a culture-based calibration (Prahl *et al*.,
674 1988).
675
676 Fig. 6. Changes in sinking flux of alkenones (kinked line), $U^{K'}_{37}$-based temperature
677 (open circle) in 1998 at 39°N, 147°E (Yamamoto *et al*., 2007), and the flux-weighted
678 annual average $U^{K'}_{37}$-based temperatures (closed circles) calculated if we assume that the
679 onset of alkenone production is delayed month by month.
680
681 Fig. 7. Schematic diagrams showing the development of an alluvial fan and changes in
682 the erosion and transportation of terrestrial soil and organic debris to study site in
683 response to marine transgression since the last glacial maximum. Arrow thickness
684 indicates the amount of transportation.
685

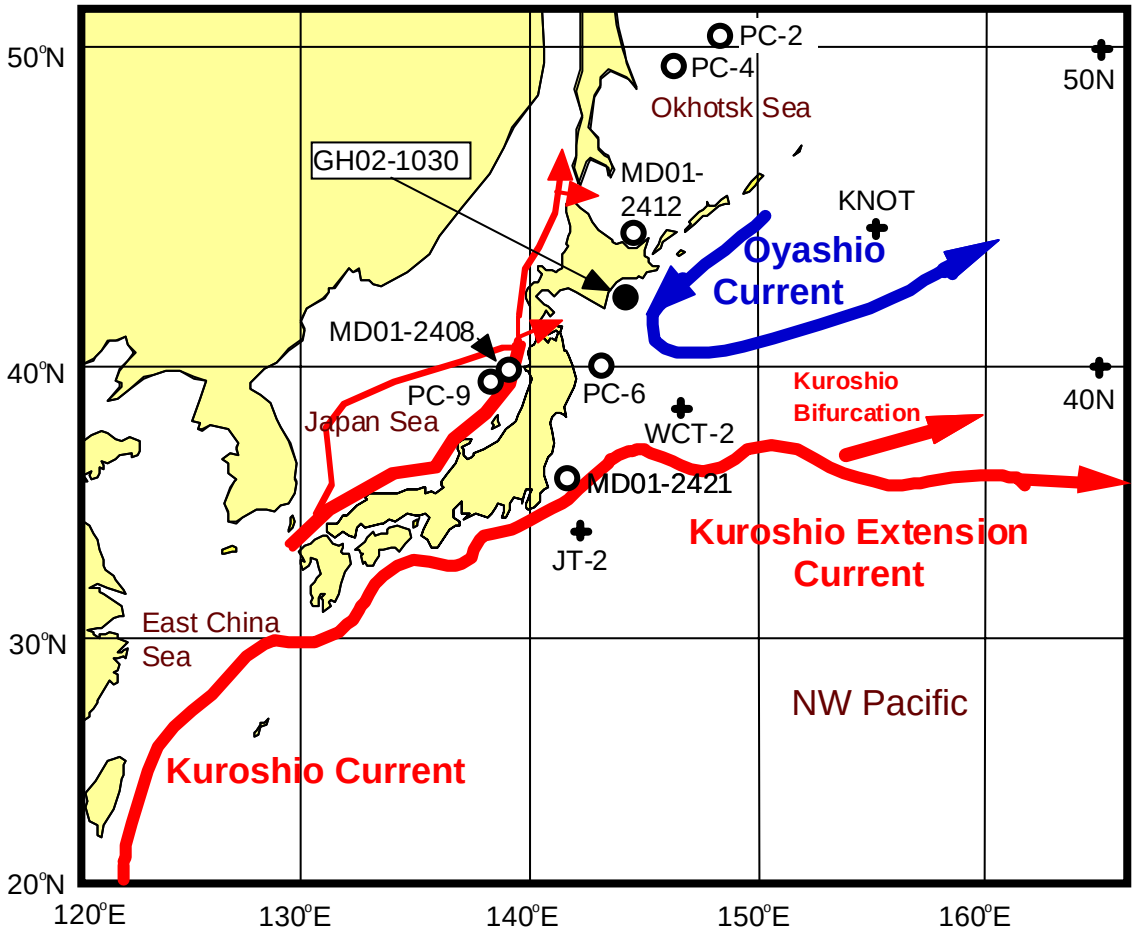

686

687 Fig. 1

688

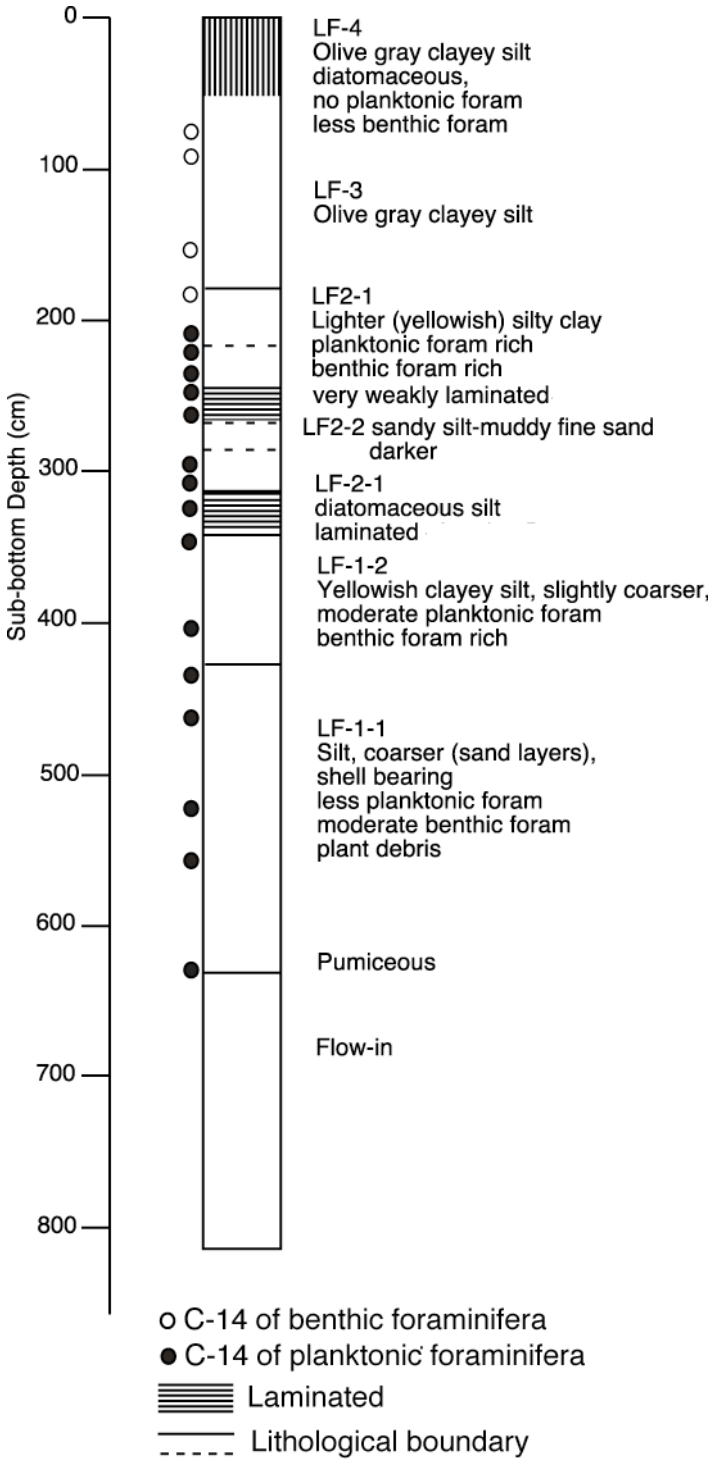

689

690 Fig. 2

691

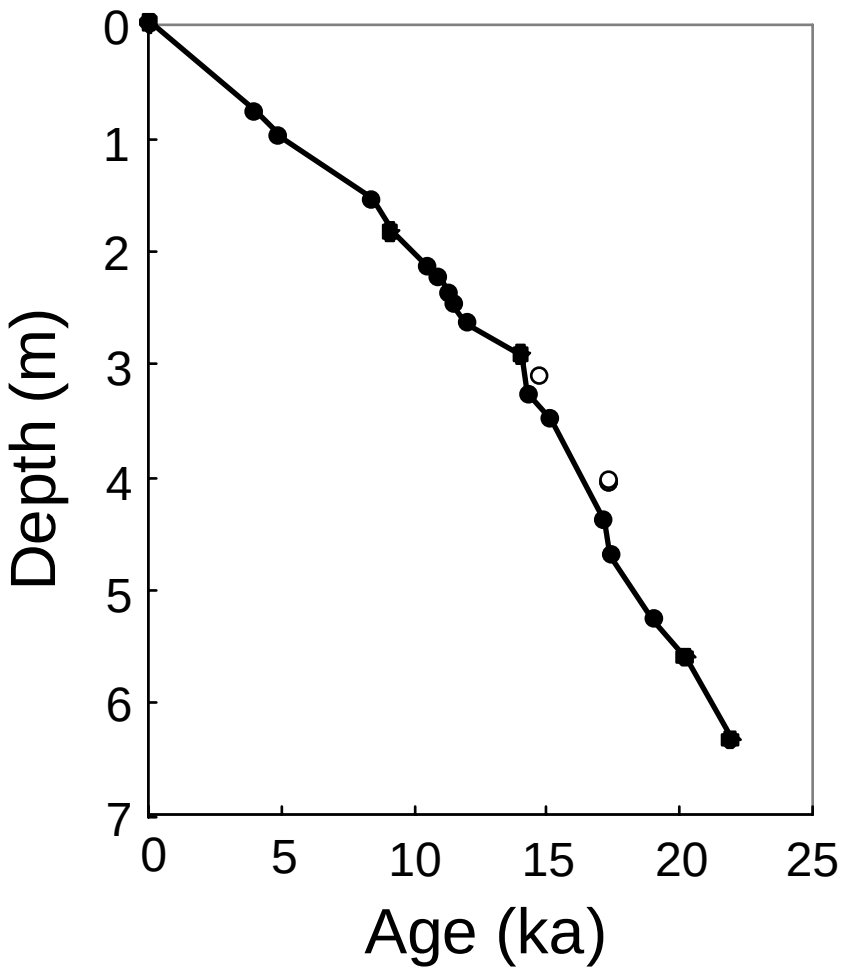

692

693 Fig. 3

694

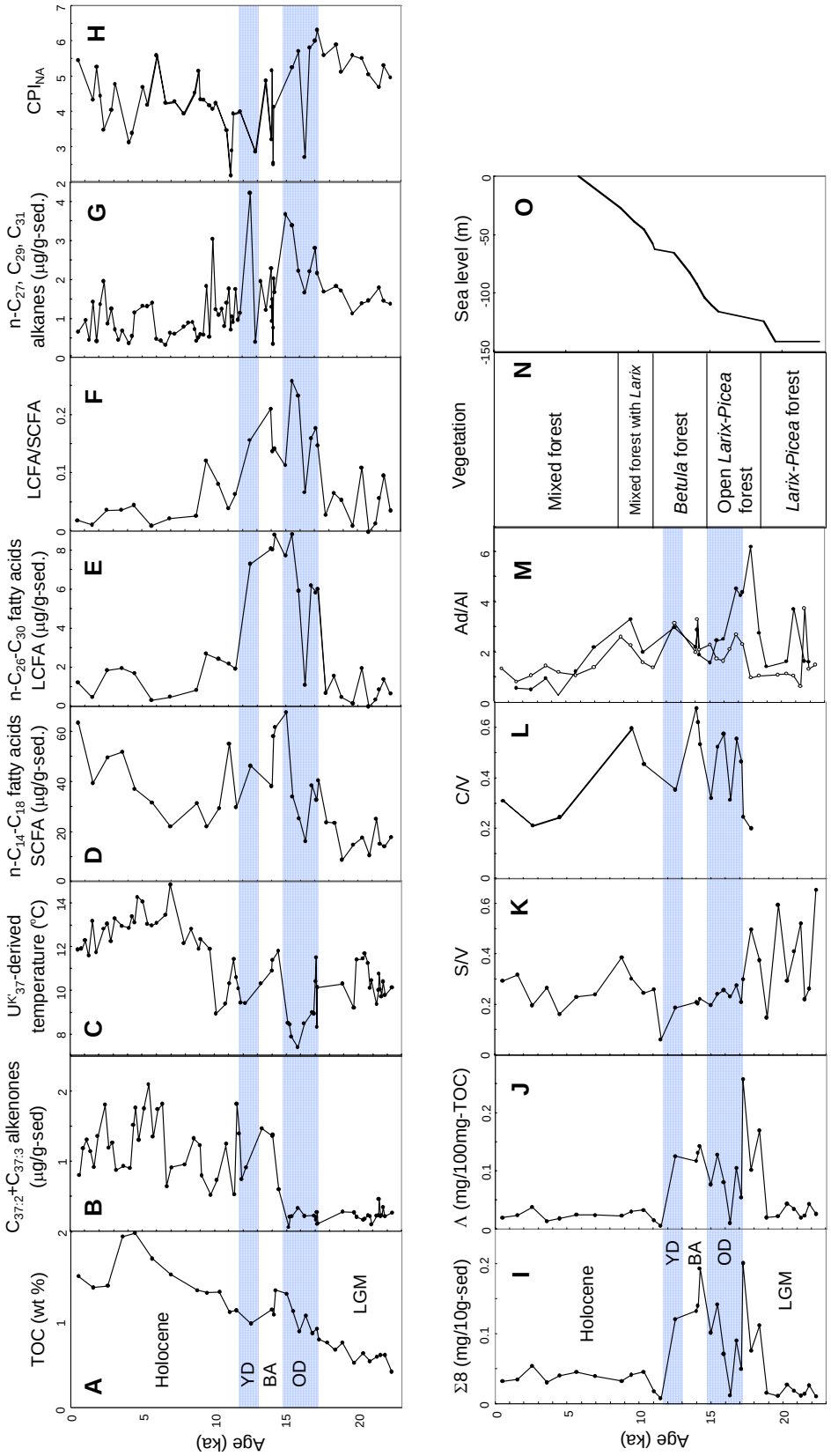
A
TOC (wt %)
Holocene
YD
BA
OD
LGM
B
$C_{37:2}$+$C_{37:3}$ alkenones (µg/g-sed)
C
$U^{K'}_{37}$-derived temperature (°C)
D
n-C_{14}-C_{18} fatty acids SCFA (µg/g-sed.)
E
n-C_{26}-C_{30} fatty acids LCFA (µg/g-sed.)
F
LCFA/SCFA
G
n-C_{27}, C_{29}, C_{31} alkanes (µg/g-sed.)
H
CPI_{NA}
Age (ka)
I
Σ8 (mg/10g-sed)
J
Λ (mg/100mg-TOC)
K
S/V
L
C/V
M
Ad/Al
Vegetation
N
Mixed forest
Mixed forest with *Larix*
Betula forest
Open *Larix-Picea* forest
Larix-Picea forest
O
Sea level (m)
Age (ka)

695

696 Fig. 4

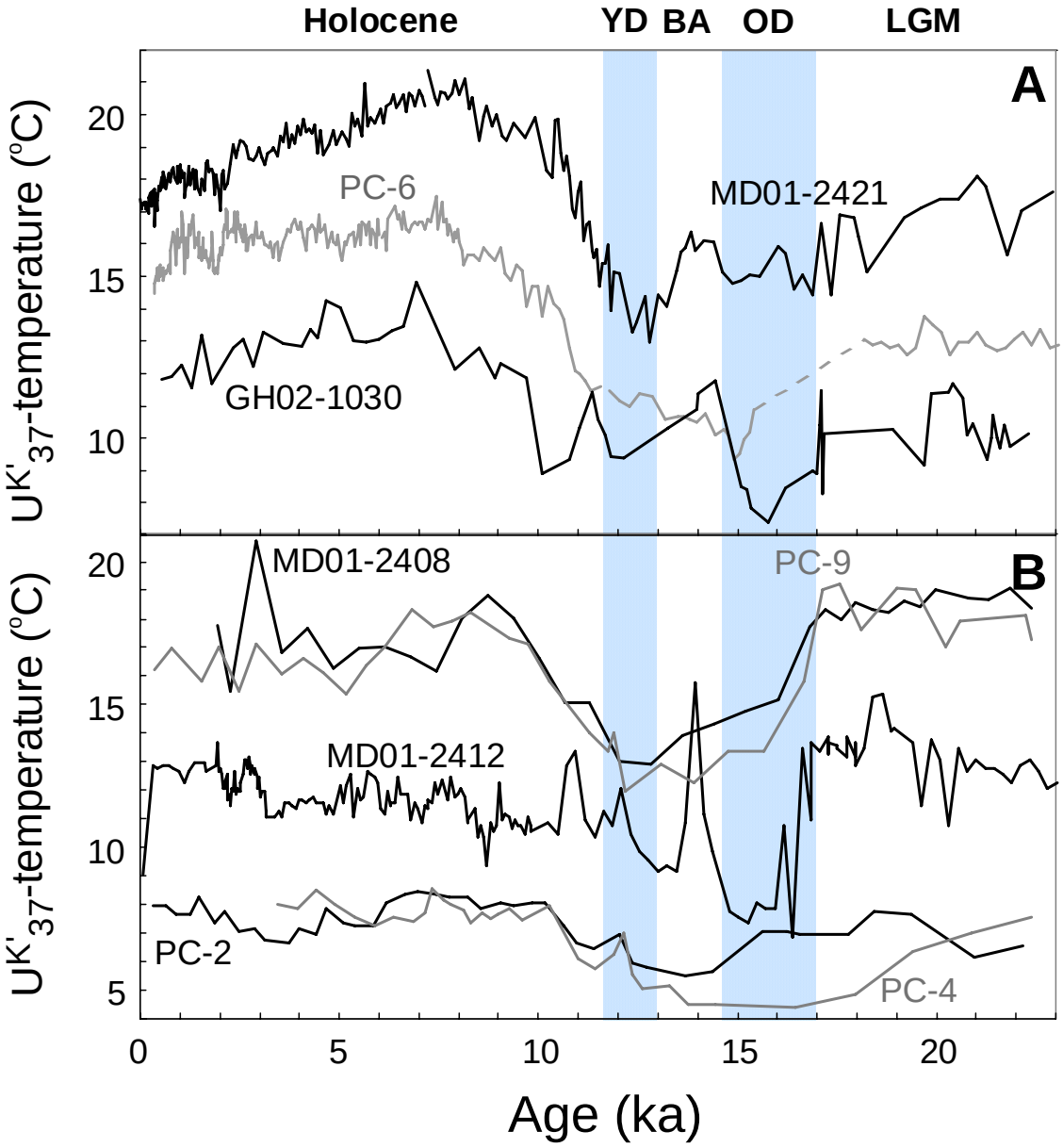
Holocene
YD
BA
OD
LGM
A
B
PC-6
MD01-2421
GH02-1030
MD01-2408
PC-9
MD01-2412
PC-2
PC-4
UK'37-temperature (°C)
Age (ka)
0
5
10
15
20

697

698 Fig.5

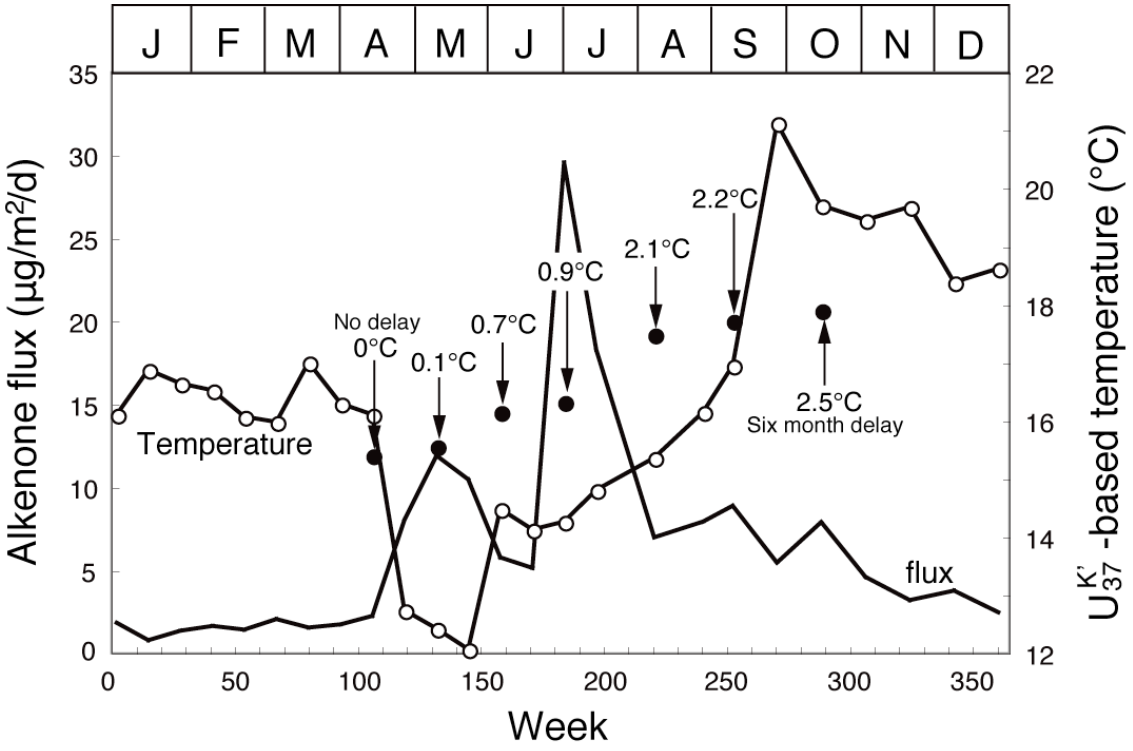
J
F
M
A
M
J
J
A
S
O
N
D
Alkenone flux (µg/m²/d)
$U^{K'}_{37}$ -based temperature (°C)
Week
Temperature
flux
No delay
0°C
0.1°C
0.7°C
0.9°C
2.1°C
2.2°C
2.5°C
Six month delay

699

700 Fig 6

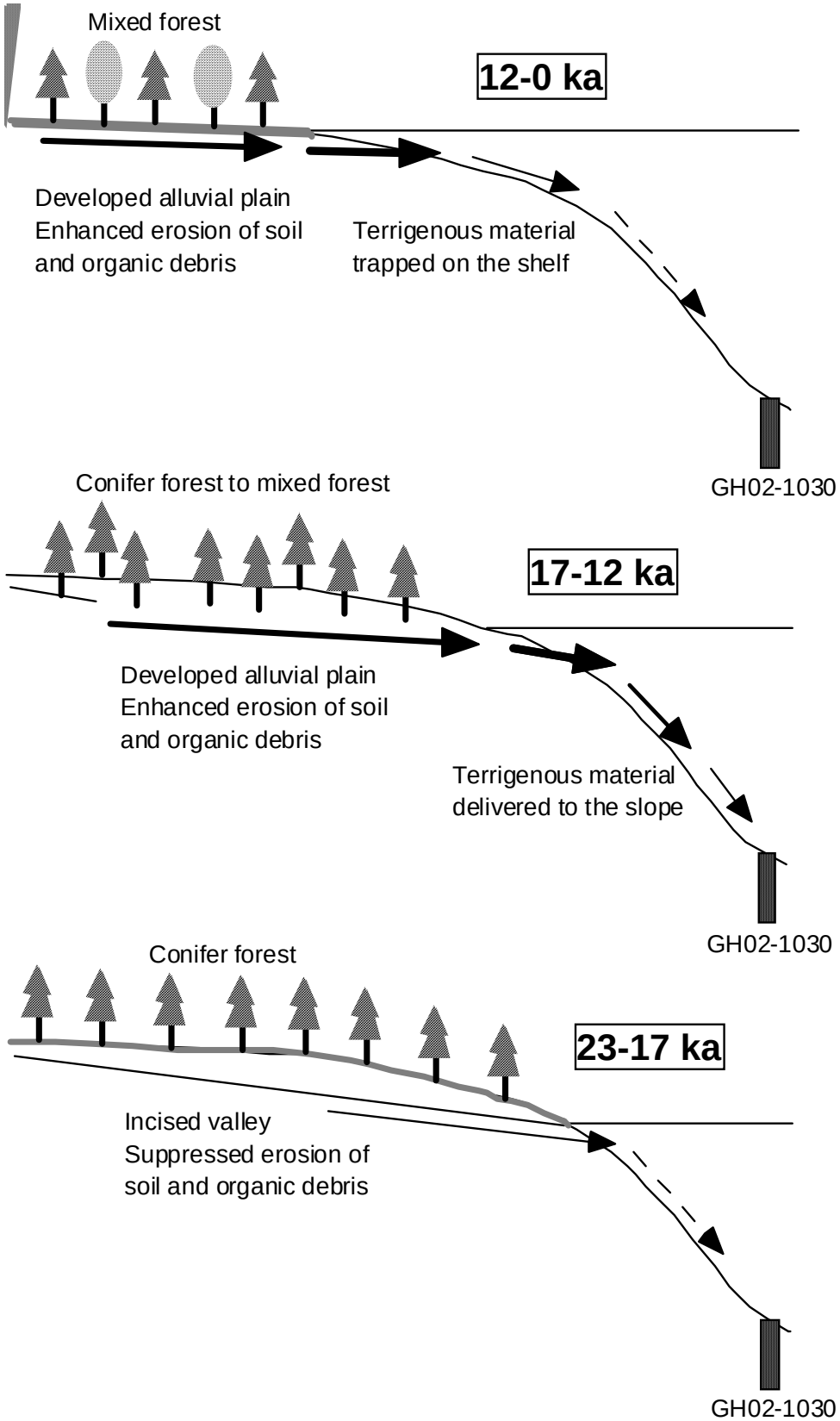
Mixed forest
12-0 ka
Developed alluvial plain
Enhanced erosion of soil
and organic debris
Terrigenous material
trapped on the shelf
GH02-1030
Conifer forest to mixed forest
17-12 ka
Developed alluvial plain
Enhanced erosion of soil
and organic debris
Terrigenous material
delivered to the slope
GH02-1030
Conifer forest
23-17 ka
Incised valley
Suppressed erosion of
soil and organic debris
GH02-1030

701

702 Fig. 7